LOAD DISTRIBUTION BEHAVIOR ON BOLTS IN DIFFERENT JOINTS CONFIGURATIONS USING THE FINITE ELEMENT METHOD

Bruno Mikio Fujiwara Marques, bmikio@yahoo.com.br
Fernando de Azevedo Silva, fazevedo@feg.unesp.br
Department of Mechanical Engineering, UNESP – Universidade Estadual Paulista, Guaratinguetá, São Paulo, Brazil

Abstract. *In this work, in order to analyze the load distribution on bolted joints, three different configurations of joints were modeled using the finite element method - FEM, varying the joined parts and shim thickness, the intensity of the applied loads and the bolt diameter. All the proposed models are bi-dimensional, modeled with plate elements which present the same inertial moment of the parts in bending condition and the contacts are modeled using spring elements. Moreover, the models take into account the hypothesis the bolt pre-load is sufficient to ensure the contact between the parts and there is no gap between the plates and the bolt. Finally, the results of the spring elements are compared with the conventional calculation method in order to demonstrate the load distribution behavior i.e., triangular, trapezoidal or rectangular.*

Keywords*: Bolted joint, FEM, load distribution, bolt*

1. INTRODUCTION

In the aeronautical industry, bolted joints are widely used and in order to control structural fit-up gap, to maintain contour or alignment, shims are used between the parts will be joined. Normally the bolts are submitted to tension and shear loads which the last one leads bending moment in the bolt due the bearing effect with the hole surface. The behavior of the load distribution in the bolt has a great contribution on its dimensioning principally because the arm that will determine the bending moment. Some bibliographies like Bruhn (1973) and Shigley, consider a rectangular load distribution behavior (Fig. 1) on the bolt in order to be conservative for the bending analysis once the distance between the applied load and the most critical section will be greater than trapezoidal or triangular load distribution behavior.

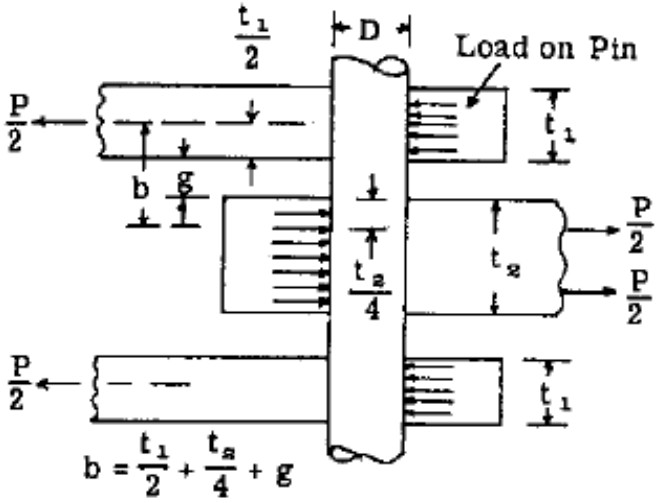

Figure 1. Rectangular load distribution in accordance with Bruhn (1973)

On the other hand, applying this conservative method, the joint may be penalized becoming a non optimized structure. Thus, in order to obtain a better joint configuration, i.e., low weight and an appropriated manufacturing and purchase cost, the others two kind of load distribution behavior are frequently applied (Fig. 2).

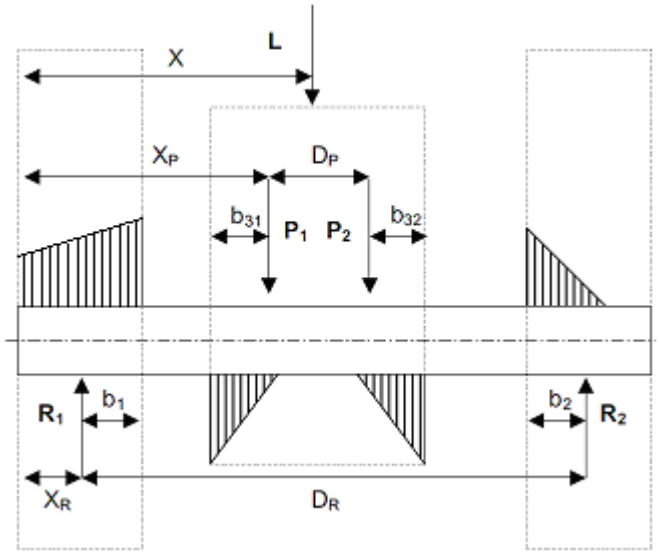

Figure 2. Trapezoidal and triangular load distribution

Therefore, this paper has the purpose to demonstrate by the finite element method the accuracy of the analytical calculation to determine what kind of load distribution behavior shall be applied on the bolt depending on the load intensity, joined parts thickness and the bearing allowables of the involved materials.

There are different ways to generate a finite element model of a bolted joint. For this study, all the proposed models are modeled using plate elements to represent the joined parts and the bolt and unidirectional spring elements to simulate the contact between the involved parts. This approach provides consistent results and takes less computational time and memory usage.

2. ANALYTICAL METHOD

The most of analytical method in order to dimension a bolted joint regarding the bolt bending strength, consider an approximate bending arm which is simply determined once the bearing forces distribution is judged uniform. In accordance with Bruhn (1973), the arm is defined by the Eq. (1) for single shear and Eq. (2) for double shear:

$$b = \frac{t_1}{2} + \frac{t_2}{2} + g \tag{1}$$

$$b = \frac{t_1}{2} + \frac{t_2}{4} + g \tag{2}$$

Where: b – bending arm
t_1 - part 1 thickness
t_2 - part 2 thickness
g – gap between the parts or shim thickness

Although, Niu (2005) mentions as the pin bends, the stress distribution tends to peak rather than form an even distribution as mentioned above.

This variation along the contact between bolt and hole leads to a triangular or trapezoidal load distribution which reduce the arm and consequently the bending stress.

The load distribution behavior depends on the thickness of the joined parts, the bolt diameter and the bearing allowables of the involved materials. For this study, the configuration is a single shear bolted joint which is demonstrated in the Fig. 3 with the involved parameters in the method.

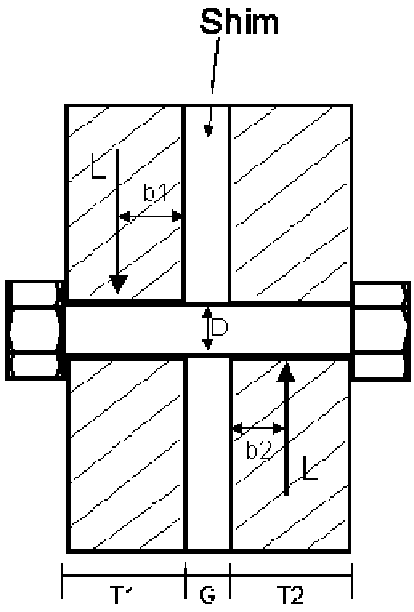

Figure 3. Bolted joint configuration

Where: b1 – distance from the applied load to plate 1 edge
b2 – distance from the applied load to plate 2 edge
T1 - part 1 thickness
T2 - part 2 thickness
G – shim thickness

First, it is considered a triangular load distribution and the maximum stress is the minimum bearing allowable among the joined parts and the bolt. See Fig. 4.

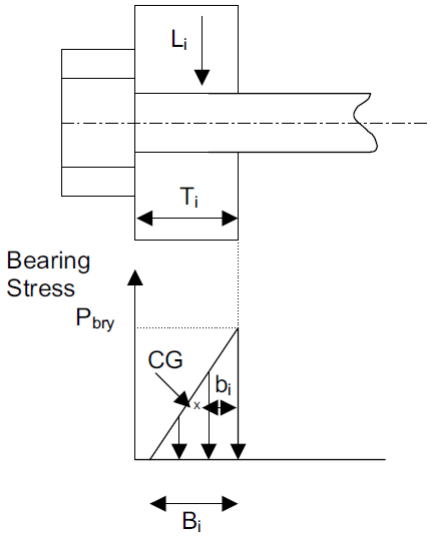

Figure 4. Triangular stress distribution

From Fig. 4, if D is the bolt diameter, the reaction on the bolt can be written as follows:

$$L = \frac{Pbry \times Bi}{2} \times D \tag{3}$$

Where *Pbry* is the minimum bearing allowable among the joined parts and the bolt and *Bi* is the length of the load distribution. And hence,

$$Bi = \frac{2 \times L}{Pbry \times D} \tag{4}$$

The value of *bi* depends on the length obtained for *Bi*:
If $Bi \leq Ti$, it is assumed there is a triangular load distribution and *bi* will be:

$$bi = \frac{Bi}{3} \tag{5}$$

If $Bi > Ti$, the load distribution may be trapezoidal or rectangular.

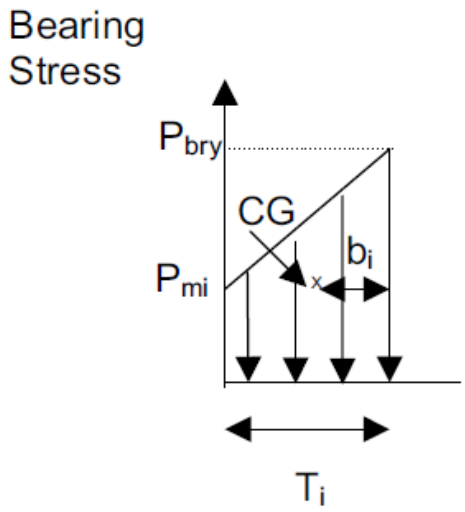

Figure 5. Trapezoidal stress distribution

From Fig. 5, the reaction on the bolt can be written as follows:

$$L = \frac{Pbry + P\min}{2} \times Ti \times D \tag{6}$$

Thus,

$$P\min = \frac{2 \times Li}{Ti \times D} - Pbry \tag{7}$$

If $Pmin \geq Pbry$, plastic deformation (or failure in ultimate condition) occurs and the load distribution becomes uniform presenting a rectangular behavior. Consequently, *bi* will be:

$$bi = \frac{Ti}{2} \tag{8}$$

However, if $Pmin < Pbry$, the load distribution will present a trapezoidal behavior and *bi* will be:

$$bi = \frac{Ti}{3} \times \left(\frac{Pbry + 2 \times P\min}{Pbry + P\min} \right) \tag{9}$$

Therefore, this study regards three different configurations of single shear bolted joints. Table 1 presents them below.

Table 1. Configurations of the bolted joints

Configuration	Bolt	D (mm)	Material – Plate 1	T1 (mm)	Material – Plate 2	T2 (mm)	G (mm)	L (N)
1	NASM21134	11.09	Al7475-T7351	12.0	Al7475-T7351	9.0	2.0	40000
2	NASM21134	6.35	Al7475-T7351	4.0	Al7475-T7351	3.0	2.5	13333
3	NASM21134	12.68	AISI4130N	11.0	Al7050-T7451	21.0	0	62867

Moreover, a FEM analysis was done respecting the three configurations above, in accordance with section 3.

3. FEM ANALYSIS

In this work, in order to generate a finite element model for the structure with a bolted joint, three kinds of bolt models are introduced in accordance with Tab. 1. All the proposed models are bi-dimensional, i.e., the bolt and joined parts are modeled with plate elements, called CQUAD4 in NASTRAN. In view of the fact that the bending behavior is the principal interest, the equivalent thicknesses of the involved components must guarantee the same inertial moment of the original sections. Thus, the formulas to define the thicknesses are:

- Bolt body

$$I = \frac{\pi \times d^4}{64} = \frac{t_b \times d^3}{12} \Rightarrow t_b = \frac{3 \times \pi \times d}{16} \tag{10}$$

Where I is the inertial moment, d is the bolt body diameter and t_b is the plate element thickness.

- Bolt head and nut

$$I = \frac{\pi \times D^4}{64} = \frac{t_{hn} \times D^3}{12} \Rightarrow t_{hn} = \frac{3 \times \pi \times D}{16} \tag{11}$$

Where I is the inertial moment, D is the bolt head or nut diameter and t_{hn} is the plate element thickness.

- Joined parts (plates)

$$I = \frac{d \times h^3}{12} - \frac{\pi \times d^4}{64} = \frac{t_p \times h^3}{12} - \frac{t_p \times d^3}{12} \Rightarrow t_p = \frac{d \times h^3 - \left(\frac{3 \times \pi \times d^4}{16} \right)}{h^3 - d^3} \tag{12}$$

Where I is the inertial moment, d is the bolt body diameter, t_p is the plate element thickness and h is the plate length.

Table 2 shows the thicknesses for each configuration.

Table 2. Model thicknesses

Configuration	d (mm)	D (mm)	h (mm)	t_b (mm)	t_{hn} (mm)	t_p (mm)
1	11.09	20.74	60.00	6.54	12.22	11.13
2	6.35	11.94	60.00	3.74	7.03	6.35
3	12.68	24.00	40.00	7.47	14.14	12.85

Moreover, the contact between the parts is modeled with unidirectional spring element, called CELAS2 in NASTRAN. For the bolt body and the joined parts, the contact stiffness is in the y direction. On the other hand, between the bolt head and the plate, between the plates and shim and between the plate and nut, the contact stiffness is in the x direction (see Fig.6). The stiffness value assumed for the contact is 10^6 N/mm and is satisfactory to obtain the load distribution on the bolt.

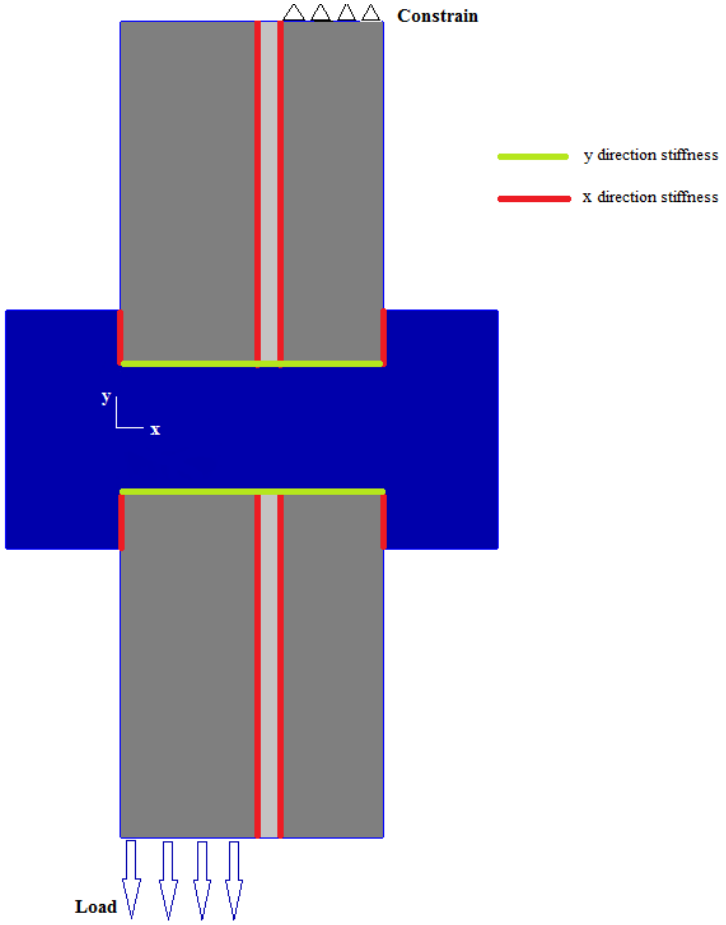

Figure 6. Contact stiffness direction

The load is applied on one edge of the plate and the degrees of freedom ux, uy and θz are constrained on the opposite edge of the other plate. Furthermore, the DOF's uz, θx and θy are constrained on all model nodes.

4. RESULTS AND DISCUSSION

The three bolted joints configurations were analyzed by the analytical method (Section 2) and FEM analysis (Section 3). In order to obtain the results from the analytical formulas, a Microsoft Excel spreadsheet was developed. Table 3 shows the results and the type of the load distribution for each configuration.

Table 3. Analytical method results

Configuration	$Pbry_1$ (MPa) (1)	$Pbry_2$ (MPa) (1)	$Pbry_{bolt}$ (MPa) (1)	B_1 (mm)	B_2 (mm)	$Pmin_1$ (MPa)	$Pmin_2$ (MPa)	b_1 (mm)	b_2 (mm)	Load distribution 1	Load distribution 2
1	695.90	695.90	2383.94	10.36	10.36	N/A	105.52	3.45	3.39	Triangular	Trapezoidal
2	695.90	695.90	2383.94	6.03	6.03	353.87	703.83	1.78	1.50	Trapezoidal	Rectangular
3	888.10	730.34	2383.94	11.17	13.59	13.70	N/A	3.72	4.53	Trapezoidal	Triangular

(1): MMPDS-04, 2008.

In accordance with Tab. 3, the joint configurations 1 and 3 present a triangular or trapezoidal load distribution while the configuration 2 presents a rectangular load distribution on plate 2. This behavior on the second joint configuration represents the beginning of plastic deformation on the plate once $Pmin_2$ surpass $Pbry_2$.

As mentioned before, the finite elements models simulate the contacts between the parts by unidirectional spring elements. After the models running, these elements provide the spring forces which can demonstrate the load distribution behavior along the bolt. Table 4 shows the spring forces from the contact between the bolt body and the plates for configuration 1.

Table 4. Spring forces for configuration 1

Spring ID	x position (mm)	y position (mm)	Spring force (N)
894	0	5.5	-4164.59
895	3	5.5	-2127.44
896	6	5.5	4407.88
897	9	5.5	15024.30
898	12	5.5	16859.87
899	14	5.5	-16302.50
900	17	5.5	-13666.51
901	20	5.5	-2717.51
902	23	5.5	2687.24
893	0	-5.5	-4164.68
892	3	-5.5	-2127.51
891	6	-5.5	4407.89
890	9	-5.5	15024.36
889	12	-5.5	16859.93
888	14	-5.5	-16302.83
887	17	-5.5	-13666.97
886	20	-5.5	-2717.86
885	23	-5.5	2686.96

From the spring ID 894 to 902, the negative values indicate there is no contact between the parts, i.e., the gap is increasing. On the other hand, from the spring ID 885 to 893, the negative values indicate the contact between the parts, i.e., there is no gap between them. Thus, the load distribution on the bolt is demonstrated on Fig. 7.

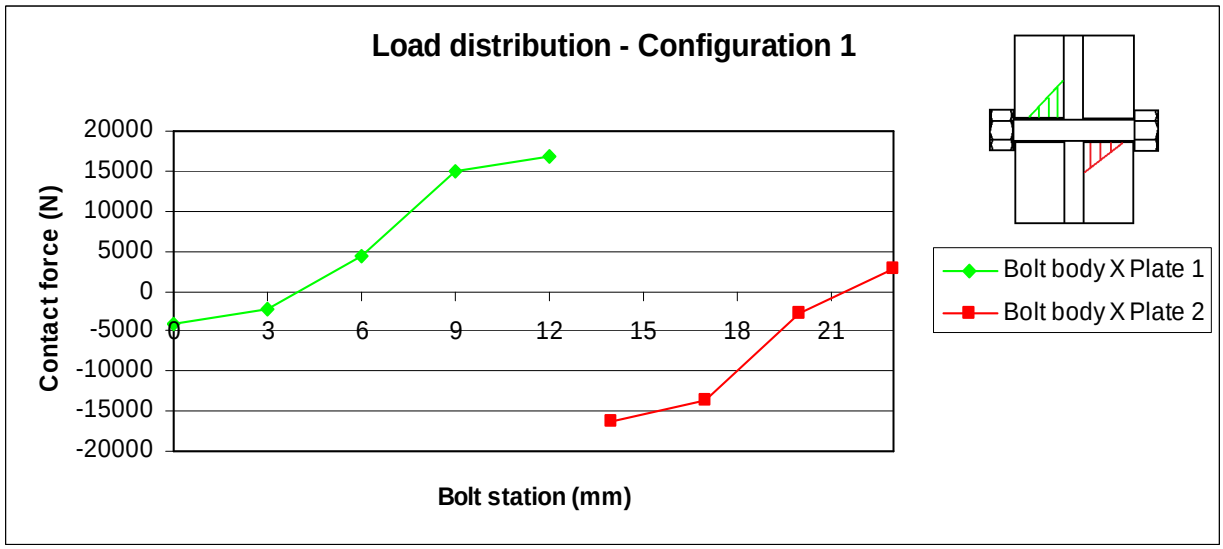

Figure 7. Load distribution – configuration 1

The results show a typical triangular load distribution behavior on the interface bolt/plate 1 and bolt/plate2. The B_1 and B_2 value from the FEM analysis are 8.03 and 7.51 mm respectively. Consequently, b_1 is 2.67 mm and b_2 is 2.50 mm.

Table 5 shows the spring forces from the contact between the bolt body and the plates for configuration 2.

Table 5. Spring forces for configuration 2

Spring ID	x position (mm)	y position (mm)	Spring force (N)
2132	0.0	3.18	469.33
2133	0.5	3.18	1164.05
2134	1.0	3.18	1285.35
2135	1.5	3.18	1617.23
2136	2.0	3.18	2038.89
2137	2.5	3.18	2528.48
2138	3.0	3.18	3125.51
2139	3.5	3.18	4024.77
2140	4.0	3.18	3746.35
2160	6.5	-3.18	-1475,184
2159	7.0	-3.18	-1259,545
2158	7.5	-3.18	-839,7566
2157	8.0	-3.18	-488,0744
2156	8.5	-3.18	-209,5536
2155	9.0	-3.18	-52,97834
2154	9.5	-3.18	387,776

From the spring ID 2132 to 2140, the positive values indicate the contact between the parts, i.e., there is no gap between them. On the other hand, from the spring ID 2160 to 2154, the positive values indicate there is no contact between the parts, i.e., the gap is increasing. Thus, the load distribution on the bolt is demonstrated on Fig. 8.

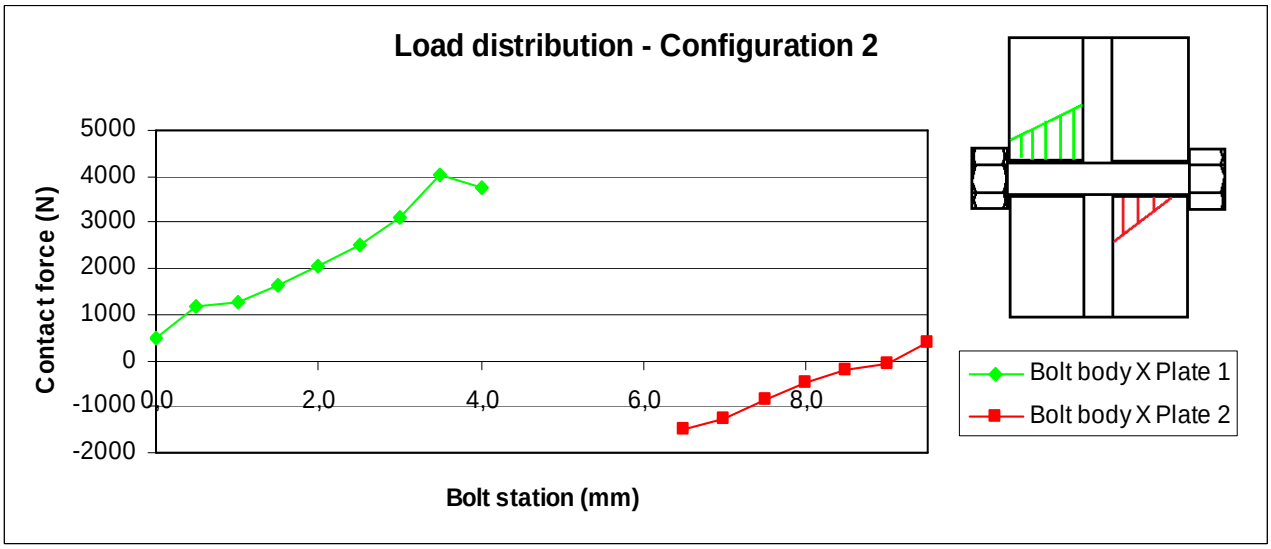

Figure 8. Load distribution – configuration 2

The results show a trapezoidal load distribution behavior on the interface bolt/plate 1 and a triangular one on the interface bolt/plate2. The B_1 and B_2 value from the FEM analysis are 4.0 and 2.6 mm respectively. Consequently, b_1 is 1.47 mm and b_2 is 0.87 mm.

Table 6 shows the spring forces from the contact between the bolt body and the plates for configuration 3.

Table 6. Spring forces for configuration 3

Spring ID	x position (mm)	y position (mm)	Spring force (N)
401	0.00	6.38	-697.10
402	2.75	6.38	3454.32
403	5.50	6.38	5466.19
404	8.25	6.38	13794.66
405	11.00	6.38	25131.94
506	11.00	-6.38	-19768.32
507	14.00	-6.38	-16194.82
508	17.00	-6.38	-8776.73
509	20.00	-6.38	-4319.24
510	23.00	-6.38	-1510.07
511	26.00	-6.38	264.73
512	29.00	-6.38	1232.60
513	32.00	-6.38	1921.87

From the spring ID 401 to 405, the positive values indicate the contact between the parts, i.e., there is no gap between them. On the other hand, from the spring ID 506 to 513, the positive values indicate there is no contact between the parts, i.e., the gap is increasing. Thus, the load distribution on the bolt is demonstrated on Fig. 9.

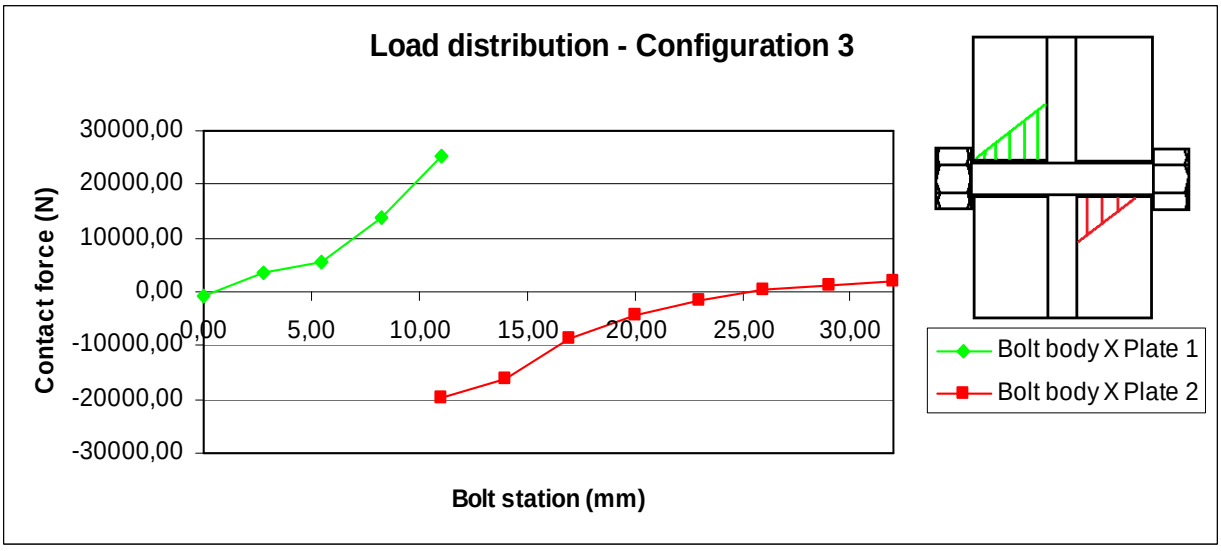

Figure 9. Load distribution – configuration 3

The results show a triangular load distribution behavior on the interface bolt/plate 1 and bolt/plate2. The B_1 and B_2 value from the FEM analysis are 10.54 and 14.55 mm respectively. Consequently, b_1 is 3.51 mm and b_2 is 4.85 mm. Figure 10 shows the configuration 3 translational displacement.

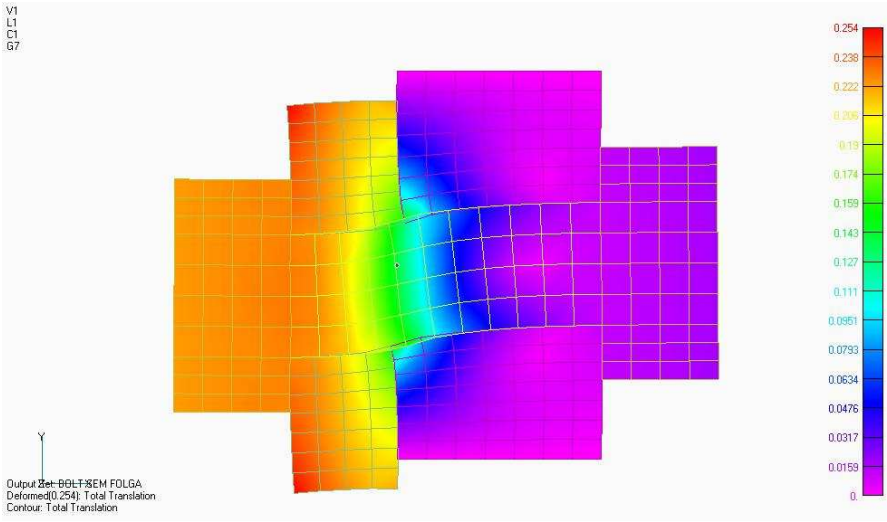

Figure 10. Translational displacement – configuration 3

Comparing the results from the analytical method and the FEM analysis, some differences come out principally for the configuration 2. For the configurations 1 and 3, the FEM analysis presented only triangular load distribution instead of the trapezoidal type obtained for some plates by the analytical method. Even though, there is a good correlation relative to the bending arm for the configuration 3, which present only 6% difference from analytical to FEM. In the case of configuration 2, the great discrepancy is on the interface bolt/plate 2 where the analytical method determined a rectangular load distribution and the FEM presented a triangular one. For this interface, the difference in the bending arm reached 72.4% and for interface bolt/plate 1 the difference is 21%.

5. CONCLUSIONS

In this paper, three different bolted joint configurations were analyzed by the analytical and finite element method. The comparison of the results confirmed the effectiveness and usefulness of the analytical method. The conclusions are summarized as the followings.

- The presence of shim in the bolted joint and the thickness of the plates influence directly the differences between the methods.
- The joint without shim and with the greatest thickness plates presented only 6% of difference because the analytical method does not regard the shim contribution and the contact stiffness defined in the FEM analysis.
- Even the difference between the methods exist, the analytical method reliability is confirmed once it can be considered all bending arms are greater than obtained in the FEM analysis. This results conservative bolted joints which will present satisfactory margin of safety and low probability of bolt failure due bending.

6. REFERENCES

Bruhn, E.F., 1973, “Analysis and Design of Flight Vehicle Structures”, 1973 Edition, University of Purdue, Purdue, USA.

MMPDS, 2008, “Metallic Materials Properties Development and Standardization”, FAA, USA, 2499 p.

Niu, M.C., 2005, “Airframe Stress Analysis and Sizing”, Second edition, Hong Kong Conmilit Press LTDA, California, USA, 795 p.

Shigley, J.E., “Elementos de Máquinas 1”, LTC Editora LTDA, Rio de Janeiro, Brazil, 347 p.

7. RESPONSIBILITY NOTICE

The authors are the only responsible for the printed material included in this paper.